

International Journal of Modern Physics E
 © World Scientific Publishing Company

ASTROPHYSICAL S-FACTOR FOR $^{16}\text{O}+^{16}\text{O}$ WITHIN THE ADIABATIC MOLECULAR PICTURE

ALEXIS DIAZ-TORRES

*Department of Nuclear Physics, Research School of Physical Sciences and Engineering,
 Australian National University, Canberra, ACT 0200, Australia
 alexis.diaz-torres@anu.edu.au*

LEANDRO ROMERO GASQUES

*Centro de Fisica Nuclear, Universidade de Lisboa, Av. Prof. Gama Pinto 2
 1649-003 Lisboa, Portugal
 lgasques@cii.fc.ul.pt*

MICHAEL WIESCHER

*Department of Physics and Joint Institute for Nuclear Astrophysics (JINA),
 University of Notre Dame, Notre Dame, IN 46556, USA
 mwiesche@nd.edu*

Received (received date)

Revised (revised date)

The astrophysical S-factor for $^{16}\text{O} + ^{16}\text{O}$ is investigated within the adiabatic molecular picture. It very well explains the available experimental data. The collective radial mass causes a pronounced resonant structure in the S-factor excitation function, providing a motivation for measuring the $^{16}\text{O} + ^{16}\text{O}$ fusion cross section at deep sub-barrier energies.

1. Introduction

The fusion cross section σ_{fus} at very low energies of reactions involving ^{12}C and ^{16}O is a crucial ingredient to calculate astrophysical reaction rates for different stellar burning scenarios in massive stars, in which $^{16}\text{O} + ^{16}\text{O}$ is the key reaction for the later oxygen burning phase. This cross section is usually represented by the S-factor ($S = \sigma_{fus} E e^{2\pi\eta}$, where η is the Sommerfeld parameter), as it facilitates the extrapolation of relatively high-energy fusion data because direct experiments at very low energies are very difficult to carry out. Unfortunately, there is a huge uncertainty in the S-factor resulted from the extrapolation of different phenomenological parametrizations that explain the high-energy data, as shown by Jiang et al.¹ for $^{16}\text{O} + ^{16}\text{O}$. For $^{12}\text{C} + ^{12}\text{C}$, the presence of pronounced molecular resonance structures makes it much more uncertain². These extrapolated values result in reactions rates that differ by many orders of magnitude¹. Therefore, a direct calculation of the S-factor at energies of astrophysical interest (< 3 MeV) is essential.

We report on an investigation³ of the fusion reaction $^{16}\text{O} + ^{16}\text{O}$ within the adiabatic molecular picture⁴, which is realistic at low incident energies. This is because the radial motion of the nuclei is expected to be adiabatically slow compared to the rearrangement of the two-center mean field of nucleons. In this reaction the nuclei are spherical and coupled channels effects are expected to be insignificant (the first collective excited state (3^-) of ^{16}O is at 6.1 MeV), making its theoretical description relatively simple. Furthermore, abundant experimental data⁵ exist for comparison to the model calculations.

A basic microscopical model to describe the studied reaction is the two-center shell model (TCSM), a great concept introduced (in practice) in heavy-ion physics by the Frankfurt school⁶. We have used a new TCSM⁷ based on realistic Woods-Saxon (WS) potentials. The parameters of the asymptotic WS potentials including the spin-orbit term reproduce the experimental single-particle energy levels around the Fermi surface of ^{16}O ⁷, whereas for ^{32}S the parameters of the global WS potential by Soloviev⁸ are used, its depth being adjusted to reproduce the experimental single-particle separation energies⁹. To describe fusion, the potential parameters (including those of the Coulomb potential for protons) have to be interpolated between their values for the separated nuclei and the compound nucleus. The parameters can be correlated⁷ by conserving the volume enclosed by certain equipotential surface of the two-center potential for all separations R between the nuclei.

2. Calculations and discussion

The adiabatic collective potential energy surface $V(R)$ is obtained with Strutinsky's macroscopic-microscopic method, whilst the radial dependent collective mass parameter $M(R)$ is calculated with the cranking mass formula¹⁰. For simplicity, the pairing contribution to the collective potential and radial mass is neglected. The rotational moment of inertia of the dinuclear system is defined as the product of the cranking mass and the square of the internuclear distance. The macroscopic part of the potential results from the finite-range liquid drop model¹¹ and the nuclear shapes of the TCSM⁷. The microscopic shell corrections to the potential are calculated with a novel method¹². The TCSM is used to calculate the neutron and proton energy levels³ E_i as a function of the separation R between the nuclei along with the radial coupling⁷ between these levels that appears in the numerator of the cranking mass expression,

$$M(R) = 2\hbar^2 \sum_{i=1}^A \sum_{j>A} \frac{|\langle j | \partial / \partial R | i \rangle|^2}{E_j - E_i}. \quad (1)$$

Figure 1a shows the s-wave molecular adiabatic potential (thick solid curve) as a function of the internuclear distance, which is normalized with the experimental Q -value of the reaction ($Q = 16.54$ MeV). The sequence of nuclear shapes

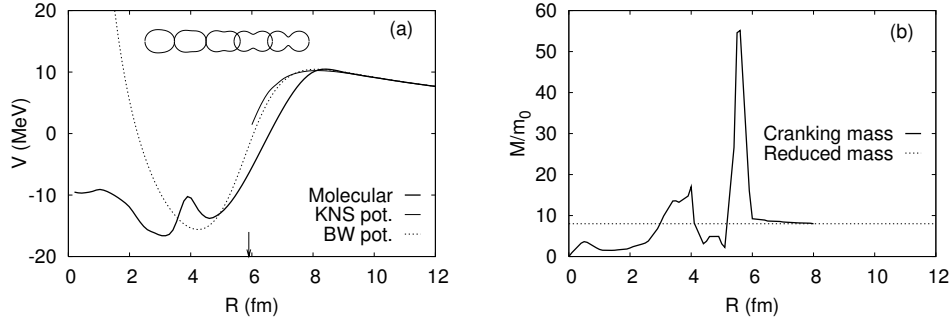


Fig. 1. (a) The s-wave collective potential energy as a function of the separation between the nuclei for $^{16}\text{O} + ^{16}\text{O}$. The arrow indicates the geometrical contact separation. (b) The radial dependent collective mass parameter (in units of nucleon mass m_0). See text for further details.

related to this potential⁷ is also presented. For comparison we show the Krappe-Nix-Sierk (KNS) potential¹³ (thin solid curve) and the empirical Broglia-Winther (BW) potential¹³ (dotted curve). Effects of neck between the interacting nuclei, before they reach the geometrical contact separation (arrow), are not incorporated into the KNS potential. The concept of nuclear shapes is not embedded in the BW potential which tends to be similar to the KNS potential. Comparing the KNS potential to the molecular adiabatic potential we note that the neck formation substantially decreases the potential energy after passing the barrier radius ($R_b = 8.4$ fm). It will be shown that the inclusion of neck effects is crucial to successfully explain the available S -factor data⁵ for the studied reaction.

Figure 1b shows the radial dependent cranking mass (thick solid curve), whilst the asymptotic reduced mass is indicated by the dotted line. Just passing the barrier radius, when the neck between the nuclei starts to develop, the cranking mass slightly increases compared to the reduced mass and pronounced peaks appear inside the geometrical contact separation. For the studied reaction, these peaks are mainly caused by the strong change of the single-particle wave functions during the rearrangement of the shell structure of the asymptotic nuclei into the shell structure of the compound system. In general, the peaks could also be due to avoided crossings⁷ between the adiabatic molecular single-particle states³, which can make the denominator of the cranking mass expression (1) very small. It is important to stress that the amplitude of these peaks may be reduced by (i) the pairing correlation that spreads out the single-particle occupation numbers around the Fermi surface, and (ii) the diabatic single-particle motion⁷ at avoided crossings, which can change those populations. For the strongest peak in Fig. 1b, which is located very close to the internal turning point for a wide range of sub-barrier energies, only aspect (i) may be relevant as the radial velocity of the nuclei is rather small there, suppressing the Landau-Zener transitions. For compact shapes, aspect (ii) may lead to intrinsic excitation of the composite system, but this is not

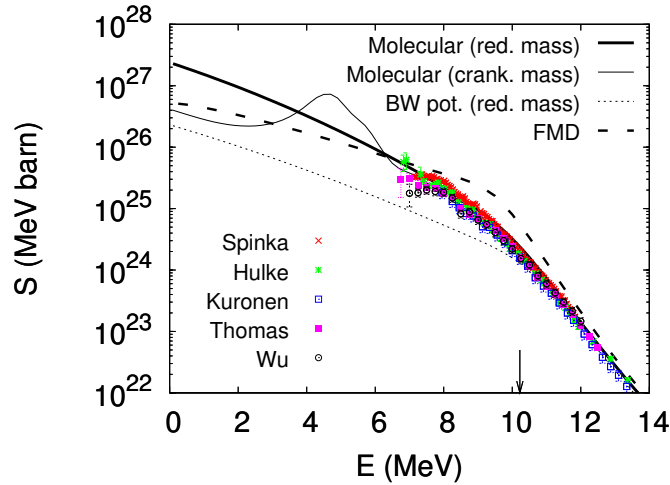
4 *Alexis Diaz-Torres, Leandro Romero Gasques and Michael Wiescher*


Fig. 2. (Color online) The S-factor as a function of the center-of-mass energy for $^{16}\text{O} + ^{16}\text{O}$. The curves are theoretical calculations, whilst the symbols refer to experimental data. The arrow indicates the Coulomb barrier of the molecular potential of Fig 1a. See text for further details.

important here for the calculation of the fusion cross section. Fusion is determined by the tunneling probability of the external Coulomb barrier, as explained below.

Having the adiabatic potential and the adiabatic mass parameter, the radial Schrödinger equation is exactly solved with the modified Numerov method and the ingoing wave boundary condition imposed inside (about 2 fm) the capture barrier. The fusion cross section σ_{fus} is calculated taken into account the identity of the interacting nuclei and the parity of the wave function for the relative motion (only even partial waves L are included here), i.e., $\sigma_{fus} = \pi\hbar^2/(2\mu E) \sum_L (2L+1)(1 + \delta_{1,2})P_L$, where μ is the asymptotic reduced mass, E is the incident energy in the total center-of-mass reference frame and P_L is the partial tunneling probability.

Figure 2 shows the S-factor as a function of the incident energy in the center-of-mass reference frame. For a better presentation, the experimental data of each set⁵ are binned into $\Delta E = 0.5$ MeV energy intervals. In this figure the following features can be observed:

- (i) the molecular adiabatic potential of Fig. 1a correctly (thick and thin solid curves) explains the measured data, in contrast to either the results obtained with the BW potential (dotted curve) or the very recent calculations within the Fermionic Molecular Dynamics (FMD) approach¹⁴ (dashed curve). Since the width of the barrier decreases for the molecular adiabatic potential of Fig. 1a, it produces larger fusion cross sections than those arising from the shallower KNS and BW potentials.
- (ii) the use of the cranking mass parameter of Fig. 1b notably affects the low

energy S-factor, which is revealed by the comparison between the thick and thin solid curves. It starts reducing the S-factor around 7-8 MeV energy region and produces a local maximum around 4.5 MeV. At the lowest incident energies (below 4 MeV) the S-factor is suppressed by a factor of five compared to that arising from a constant reduced mass. The peak in the S-factor is due to an increase of the fusion cross section, which is caused by the resonant behavior of the collective radial wave function³.

3. Concluding remarks and outlook

The adiabatic molecular picture very well explains the available experimental data for the S-factor of $^{16}\text{O} + ^{16}\text{O}$. The collective radial cranking mass causes a relevant peak in the S-factor excitation function, although the pairing correlation (neglected in the calculation) may somewhat reduce the magnitude of this bump. It is highly desirable to have fusion cross sections, measured around 4-5 MeV, to verify the existence of this resonant structure in the S-factor. The collective mass surface is very important for the reaction dynamics, and its effect on fusion of heavy-ions should be investigated systematically. This can be significant for a better understanding of reactions forming superheavy elements. Works are in progress for understanding the molecular resonance structures in the S-factor excitation function of the challenging system $^{12}\text{C} + ^{12}\text{C}$.

Acknowledgements

This work was supported by the Joint Institute for Nuclear Astrophysics (JINA) through grant NSF PHY 0216783, and by an ARC Discovery grant.

References

1. C.L. Jiang et al., *Phys. Rev. C* **75** (2007) 015803.
2. E.F. Aguilera et al., *Phys. Rev. C* **73** (2006) 064601.
3. A. Diaz-Torres, L.R. Gasques and M. Wiescher, *Phys. Lett. B* **652** (2007) 255.
4. W. Greiner, J.Y. Park and W. Scheid, in *Nuclear Molecules* (World Scientific, Singapore, 1994).
5. H. Spinka and W. Winkler, *Astrophys. J.* **174** (1972) 455; G. Hulke, C. Rolfs and H.P. Trautvetter, *Z. Phys. A* **297** (1980) 161; A. Kuronen, J. Keinonen and P. Tikkanen, *Phys. Rev. C* **35** (1987) 591; J. Thomas et al., *Phys. Rev. C* **33** (1986) 1679; S.C. Wu and C.A. Barnes, *Nucl. Phys. A* **422** (1984) 373.
6. P. Holzer, U. Mosel and W. Greiner, *Nucl. Phys. A* **138** (1969) 241; J.A. Maruhn and W. Greiner, *Z. Phys.* **251** (1972) 431.
7. A. Diaz-Torres and W. Scheid, *Nucl. Phys. A* **757** (2005) 373.
8. V.G. Soloviev, in *Theory of Complex Nuclei* (Pergamon Press, Oxford, 1976) p. 21.
9. G. Audi and A.H. Wapstra, *Nucl. Phys. A* **565** (1993) 1.
10. D.R. Inglis, *Phys. Rev.* **103** (1956) 1786.
11. P. Möller and J.R. Nix, *Atomic Data and Nuclear Data Tables* **26** (1981) 165.
12. A. Diaz-Torres, *Phys. Lett. B* **594** (2004) 69.
13. W. Reisdorf, *J. Phys. G* **20** (1994) 1297.

6 *Alexis Diaz-Torres, Leandro Romero Gasques and Michael Wiescher*

14. T. Neff, H. Feldmeier and K. Langanke, arXiv: nucl-th/ **0703030**.